Daniel Flamm, Marc Sailer, Daniel Günther Grossmann, Steffen Rübling, Dennis Decker, Christian Gaida, Markus Blothe, Dirk Sutter, and Stefan Nolte "Ultrafast laser micromachining using wavelengths from ∼0.2 µm to ∼2 µm", Proc. SPIE 13353, Frontiers in Ultrafast Optics: Biomedical, Scientific, and Industrial Applications XXV, 1335308 (19 March 2025); https://doi.org/10.1117/12.3042674.

Invited Paper

Ultrafast laser micromachining using wavelengths from ∼ 0.2 µm to ∼ 2 µm

Daniel Flamm,[a] Marc Sailer,[b] Daniel Günther Grossmann,[b] Steffen Rübling,[b] Dennis Decker,[a] Christian Gaida,[c] Markus Blothe,[d] Dirk Sutter,[b] and Stefan Nolte[d,e]

[a]TRUMPF Laser- und Systemtechnik GmbH, 71254 Ditzingen, Germany
[b]TRUMPF Laser GmbH, 78713 Schramberg, Germany
[c]Active Fiber Systems GmbH, 07745 Jena, Germany
[d]Friedrich Schiller University Jena, Institute of Applied Physics, Abbe Center of Photonics, 07745 Jena, Germany
[e]Fraunhofer Institute for Applied Optics and Precision Engineering IOF Jena, Center of Excellence in Photonics, 07745 Jena, Germany

ABSTRACT

We review micromachining strategies with optimized energy deposition from ultrafast lasers operating with wavelengths from 1980 nm down to 257 nm. By discussing multifarious machining concepts, such as, e.g., in-volume silicon processing (NIR), drilling of fine-metal masks (green), or cutting of polymer foils (DUV), we show how processing benefits from adapted photon energies or tighter foci. In all cases, an optimized processing solution is achieved precisely when light source, beam shaping and focusing concept are tailored to each other and to the respective light-material interaction.

Keywords: Ultrafast optics, laser materials processing, micromachining, structured light, colored lasers, ultraviolet lasers, deep-ultraviolet lasers, frequency conversion, thulium lasers, light-matter-interaction

1. INTRODUCTION

Modern manufacturing benefits from ultrashort laser pulses acting as subtle tools for micro- and nanomachining.[1–3] Here, highest spatiotemporal photon densities enable interaction with all conceivable materials, independent of the state of matter or absorption behavior.[4–6] The industrial state of the art in terms of the light source are ytterbium-based lasers in various amplifier geometries operating at a wavelength of ∼ 1030 nm.[7–9] Prime examples for processing with such sources are cutting, drilling or ablation strategies where multi-millijoule and multi-hundred-watt laser platforms have been successfully applied.[10–12]

The goal of any laser-based materials processing strategy is to control the deposition of energy in order to create reasonable material modifications.[13,14] Here, photon energy plays a crucial role for optimizing linear absorption or for triggering a specific nonlinear material response to the pulse.[15] Using frequency-converted signals of above-mentioned lasers, radiations at ∼ 515 nm (green, frequency doubled), ∼ 343 nm (UV, frequency tripled) and ∼ 257 nm (DUV, frequency quadrupled) are available. Besides optimized interaction with the material of the workpiece, processing with shorter wavelengths benefits from tighter foci, shorter penetration depths and, thus, from more confined modifications and smaller heat-affected zones.[16]

We will review micro-processing strategies with ultrashort laser pulses operating at the above-mentioned wavelengths, such as, large-scale ablation of metals (IR-1-µm, Sec. 2), drilling of fine-metal masks (green, Sec. 3), through-hole drilling in polymer films (UV, Sec. 4) or cutting of polymer foils (DUV, Sec. 5). This menu is completed by discussing in-volume silicon processing strategies with thulium-based ultrafast lasers providing pulses at ∼ 1980 nm (IR-2-µm, Sec. 6).

The respective sections also contain information on the most important specifications of the industrial ultrashort pulsed lasers used.

Further author information:
E-Mail: daniel.flamm@trumpf.com.

© 2025 Society of Photo-Optical Instrumentation Engineers (SPIE). One print or electronic copy may be made for personal use only. Systematic reproduction and distribution, duplication of any material in this publication for a fee or for commercial purposes, and modification of the contents of the publication are prohibited.
Frontiers in Ultrafast Optics: Biomedical, Scientific, and Industrial Applications XXV © 2025 SPIE.
https://doi.org/10.1117/12.3042674.

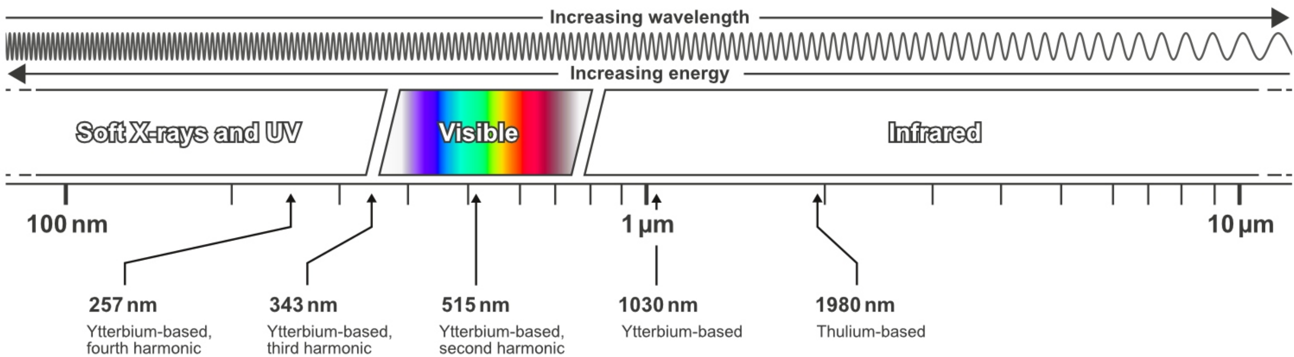

Figure 1: Classification of the five wavelengths used in this work within the electromagnetic spectrum.

2. MICROMACHINING WITH 1030 NANOMETER PULSES

Over the last two decades, solid-state lasers have almost completely replaced the established gas lasers—until then the workhorses of industrial laser production. Although there are still application strategies where the processing quality of a CO2 laser ($\lambda \approx 10\,\mu\text{m}$) is unsurpassed, e.g. when cutting thick steels,[17] the advantages of ytterbium-based lasers outweigh them. These relate in particular to efficiency, but also to maintenance, footprint and complexity. With their typical wavelength at $\lambda = 1030\,\text{nm}$ these lasers have become established for various reasons. The availability and manufacturability of highly transparent optical components for guiding (just consider the impact of optical fibers), shaping and focusing have contributed to their success, as have efficient pumping strategies with NIR laser diodes and the ability to generate sub-picosecond pulses from the active medium.[7] Ultimately, the high transparency and good thermal conductivity of the host material, such as YAG (yttrium aluminum garnet),[18] enabled the development of pulsed lasers with highest powers and energies, cf. Sec. 1.[19]

Today, ytterbium-based ultrashort pulsed lasers are available industrially, enabling peak intensities of more than 1E16 W/cm^2 (for example, when focusing a 2-mJ and 1-ps-pulse down to spot dimensions of $5\,\mu\text{m}$ using a 0.2-numerical aperture (NA).[12] Such extreme powers pose challenges if they are to be used for laser materials processing but enable orders of magnitude higher processing productivity compared to lower power ultrafast lasers.[20,21] This requires advanced optical engineering to distribute the radiation onto large areas or into large volumes, which, ultimately, enables micromachining on macroscopic dimensions.[21,22] Prime examples to mentioned strategy can be found in the single-pass cutting of centimeter-scaled architectural glass using non-diffracting beams[12,23] or the surface texturing with interference patterns.[11,24] In both examples, the processing optics is the enabler to fully exploit the power performance of the laser source.[12] To be more precise, in order to make use of the average power available, highly dynamic axis stages or scanning systems, or combinations thereof, such as polygon scanners in combination with roll-to-roll processes, are required.[20,24] On the other hand, completely exploiting the laser's pulse energy, tailored focus shapes such as non-diffracting beams[23,25] or multi-spot distributions need to be applied.[26,27] Considering diffractive beam splitting, parallel processing with hundreds of focus copies has already been demonstrated.[20,28] From an optical perspective, beam splitting is possible in $\sim (1000 \times 1000)$ focus copies in one transverse focal plane either via diffractive concepts[11,20] or by employing interference patterns.[29,30] In addition, the extension of the beam splitting approach to three spatial dimensions has already been demonstrated ("photonic shaping tool")[31] and used for volume materials processing of display glasses.[21,32]

However, since a constant growth in pulse energies for industry-grade ultrafast laser sources is expected,[33] throughput can be scaled not only by increasing the number of focus copies from beam splitting for parallel processing. An alternative is given by employing uniform focus distributions, such as line focus shapes (1D)[34] or flat-top distributions (2D).[35] The latter is already used for microdrilling of rectangular holes in thin metal foils acting as high-resolution masks for thermal OLED deposition.[3,36] Typical flat-top dimensions range from $l = (5 \ldots 50)\ \mu\text{m}$ with required edge steepness of $< l/10$,[3] cf. Sec. 3. As the processing threshold needs to be exceeded at the entire homogenized area, and not only at discrete positions (multispot case), the pulse

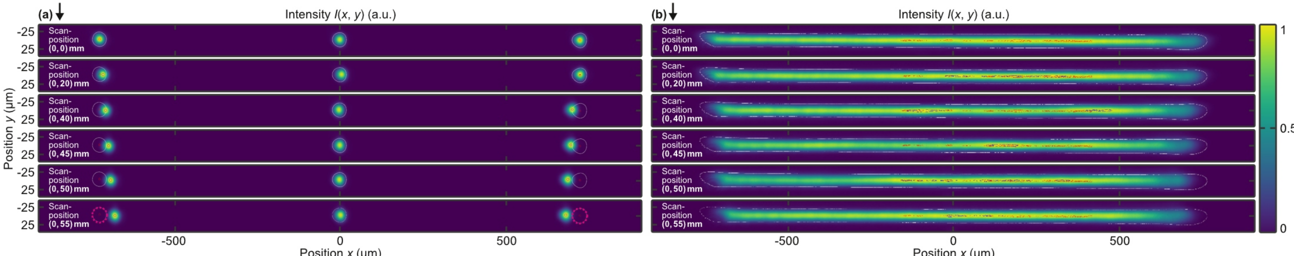

Figure 2: Measured transverse intensity distributions at scan positions $\Delta y = (0\dots55)$ mm. At increasing scan positions a decrease in the spatial dimension of the focus shapes is visible for both beam shaping concepts: beam splitting[26] (a) and beam homogenization[35] (b), caused by the induced distortion of the employed objective.

energy requirement will be higher—especially if the flat-top is scaled to macroscopic dimensions. For example, a typical ablation threshold of 1-µm-picosecond pulses on metals is $\sim 1\,\mathrm{J/cm^2}$.[5] With the envisaged 100-mJ-pulse energies,[33] squares with edge lengths of $\sim 3\,\mathrm{mm}$ could already be processed with a single pulse assuming an efficient and uniform flat-top shaping concept.

In our experiment, sub-picosecond pulses from a TruMicro 6020 laser[37] are beam shaped with a liquid-crystal-on-silicon-based spatial light modulator (SLM), guided through a Scanlab excelliSCAN 14 galvo scanner and focused with a telecentric f-θ-objective. Using phase-only modulation the SLM acts on the one hand as beam splitter and on the other as a homogenizer, see Fig. 2 (a) and (b), respectively. The quality of both focus distributions meet the demands of our applications, as the Gaussian shape of the raw beam as well as beam quality in terms of M^2-parameter are close to the theoretical limit. With an effective focal length of $f = 160\,\mathrm{mm}$ the focusing unit is illuminating the workpiece over an area of $\sim (1500 \times 25)\ \mathrm{\mu m^2}$ where beam splitting and homogenization (field mapping according to Ref. 35) is applied only to the long axis (x-axis). Using an excelliScan14 the relative movement of focus distribution and workpiece is realized based on galvanometer scanning mirrors. In Fig. 2, the performance of the focus shapes is investigated for different scan positions $\Delta y = (0\dots55)$ mm. This deflection corresponds to a fully utilized scan field of the respective optics. Towards the edges of the scanning area the measured intensity distributions exhibit a length reduction of approximately twice the spot diameter ($\sim 50\,\mathrm{\mu m}$) caused by the objective's distortion.[38] The change in focus distribution during the scanning process—negligible in the present case—shows that the beam shaping approach has to be designed taking the properties of the focusing unit and the source into account.[12]

The beam shaped foci are employed to ablate stainless steel for efficient fabrication of dimples and grooves, respectively, see Fig. 3. At an optimized fluence of $0.7\,\mathrm{J/cm^2}$ demonstration (a) shows a transverse scan of the applied beam shape with a scan speed of $8\,\mathrm{m/s}$. For the target depth of approx. $1\,\mathrm{\mu m}$, 9 passes where applied. The uniformity of the employed intensity distribution is directly transferred in a homogeneous surface treatment. A process utilizing the feed direction in the elongated axis of the intensity distribution enables alternative applications. In (c) ablation of 10-µm-grooves is conducted with a single pass at $1\,\mathrm{m/s}$. Compared to a classical multi pass ($\times 80$) Gaussian focus process in (b) at $1\,\mathrm{m/s}$, an acceleration of factor 80 (corresponding to the scaled geometry) can be achieved while improving processing quality for specific regimes. With such beam shaping methods an increased pulse energy and average laser power enable a massively increased throughput for specific applications.

This section is completed by a brief overview about the TRUMPF TruMicro laser portfolio operating at 1030 nm including specification of an industry-grade 1-kW-average power version (TruMicro 9010), see Table 1.

3. MICROMACHINING WITH 515 NANOMETER PULSES

Converting the already efficiently generated 1-µm-radiation into the green wavelength range can be achieved with efficiencies well above 50 %[40] using, for example, frequency doubling in LBO (lithium triborate) crystals meeting type I phase matching condition.[41,42] Halving the wavelength of the ytterbium-based primary laser to 515 nm by adding an external conversion module ensures that excellent laser features of the primary source, for example, with regard to the temporal pulse flexibility or spatial stability,[43] are also available for the converted

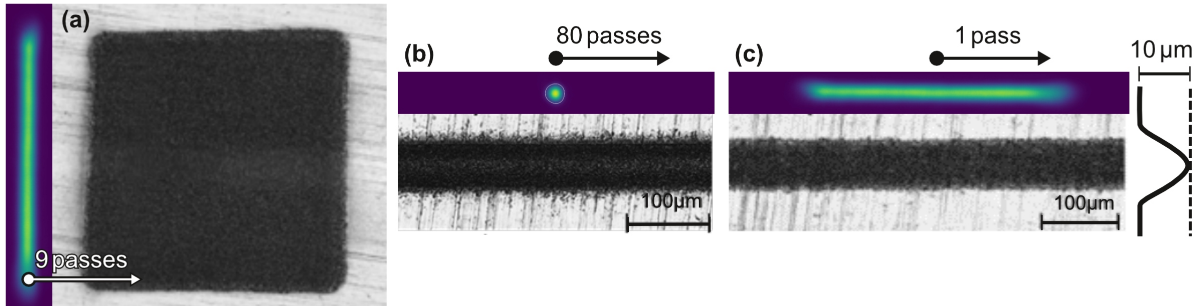

Figure 3: Processing stainless steel with flat-top-like focus distributions. In subfigure (a), feed direction was chosen perpendicular to the line focus resulting in rectangular surface treated areas of ablation depth 1 µm. In (c) a feed direction in the elongated axis enabled grooving in a single pass with an ablation depth of 10 µm.

Table 1: Examples of the TRUMPF TruMicro laser portfolio operating at $\lambda = 1030$ nm with relevant specifications.[39]

	TruMicro 6020	**TruMicro 6030**	**TruMicro 9010**
Wavelength	1030 nm	1030 nm	1030 nm
Average power (max)	200 W	300 W	1000 W
Advanced pulse on demand	up to 1 MHz	up to 1 MHz	up to 2 MHz
Repetition rate (max., single pulse picking)	2 MHz	2 MHz	2 MHz
Repetition rate (max., QCW mode)	50 MHz	50 MHz	50 MHz
Pulse energy (max.)	0.2 mJ or 2 mJ	0.2 mJ or 2 mJ	10 mJ
Burst patterns	up to 16	up to 16	up to 16
Burst energy (max.)	8 mJ	8 mJ	40 mJ
Pulse duration	850 fs	850 fs	< 1 ps
Beam quality	$M^2 < 1.3$	$M^2 < 1.3$	$M^2 < 1.3$

radiation. This is ensured by the fact that the laser system is regulated with the converted signal, i.e. the primary laser (IR) is controlled to achieve optimum performance for the secondary radiation (green). Materials processing with green ultrafast lasers already benefit from tighter foci and from enhanced absorption considering, for example, many metals[44] but also transparent materials such as stained glasses.[45] Quality advantages of the green wavelength arise when cutting printed circuit boards (PCBs), which are typically composed of layers of different materials or material mixtures such as glass fiber reinforced epoxy laminate.[46] Here, green femtosecond (fs) pulses are superior to infrared fs pulses with respect to burr and particles at the cutting edge. However, they compete with cheap nanosecond 1-µm-solutions (low-quality end) and even with UV picosecond pulses (high-quality end). Whether the increased cost of doubling the frequency is actually worthwhile and results in a more efficient processing strategy is at least controversial with respect to metal[47,48] and PCB processing,[46,49] and will depend on a number of secondary conditions, particularly considering the mentioned process quality but also use of assisting gas and the level of material fluctuations.[49]

In any case, the halved diffraction limit enables the application of advanced beam shaping concepts such as the use of micrometer-scaled flat-tops for microdrilling in thin metal foils where smallest intensity features need to be applied to the workpiece. High-resolution masks for thermal OLED deposition are required exhibiting rectangular holes with steepest edges fabricated in invar, for example.[3] As depicted in Fig. 4 (left-hand-side), we are shaping rectangular flat-tops employing a laser similar to a TruMicro 2230 providing 300-fs-pulses at $\lambda = 515$ nm. Our beam shaping concept makes use of the state-of-the-art field mapper[35] in combination with a second, amplitude filtering step.[3] These two beam shaping stages are realized with a single SLM in a double illumination design. For the first illumination the SLM's transmission is phase-only acting as field mapper. For the second one, the polarization is prepared in a way that the SLM is applying an amplitude modulation to

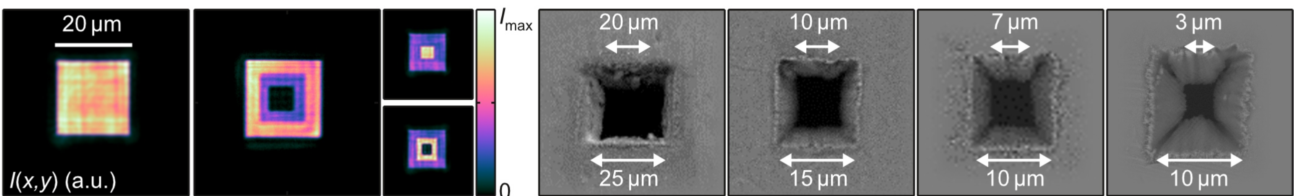

Figure 4: Controllable taper angles of drilled rectangular holes in invar foil with a thickness of 10 µm for FMM applications. Different taper angles are achieved using flat-top like beams with customized intensity gradients (left hand side).[3]

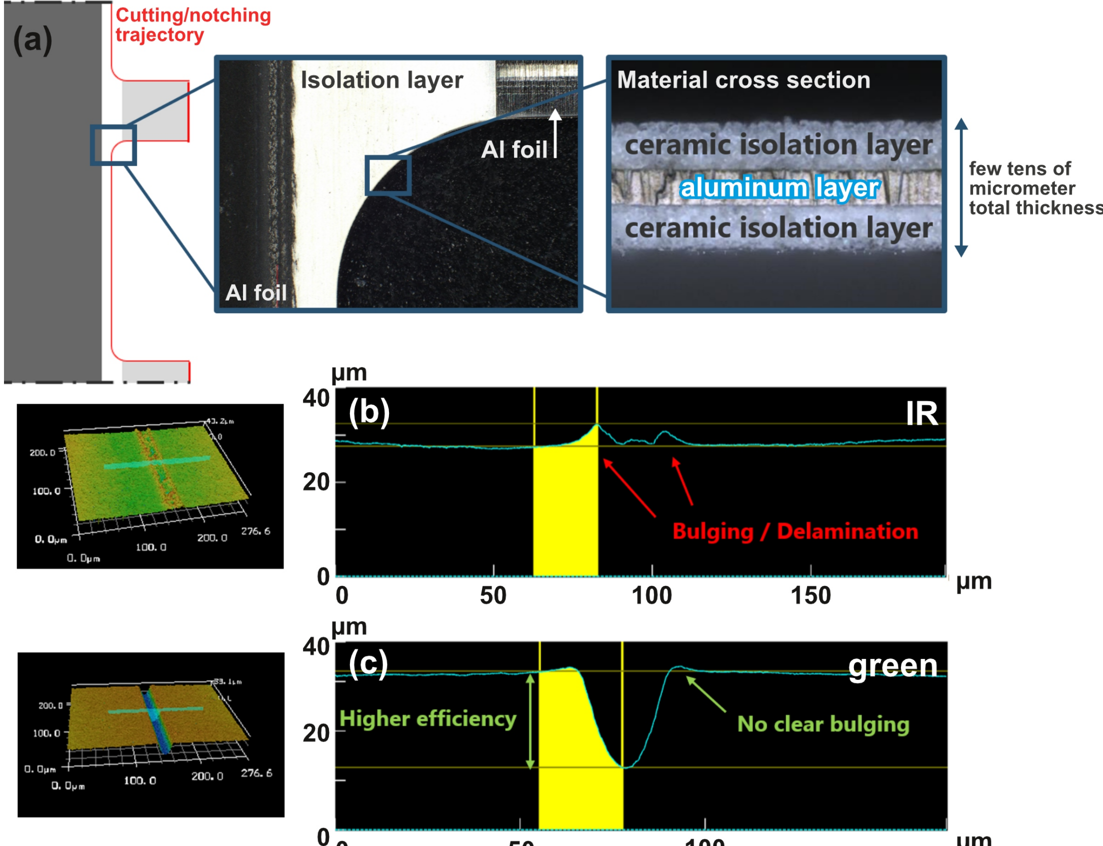

Figure 5: High-quality notching of battery isolation layers (a). When cutting the layer system composed of aluminum and the ceramic isolation layer, bulging and delamination effects occur if the absorption is inappropriate as for the 1-µm-case (b). Green femtosecond pulses, on the other hand, allow an efficient ablation of the isolation layer preventing the delamination (c).

optical field, for details see Ref. 3. As a result, flat-tops with highest edge steepnesses and edge radii in the order of 1 µm are generated using NA-0.4-focusing units. Resulting micro-drilling samples are depicted in Fig. 4 (right-hand-side) showing rectangular holes with customized taper-angles from scanning electron microscopy. Local intensity gradients of the circularly polarized flat-top-like beams enable to control the 3D hole geometry, see different entrance and exit hole dimensions. Taper angles are mainly controlled by the structured amplitude of the flat-tops resulting in local intensity gradients.

A second micromachining application for green ultrashort pulses relates to the cutting of notch contours of isolation layers used for safer production of batteries, see Fig. 5 (a). The ∼ 10-µm-thick ceramic layer surrounds the conductive aluminum foil and prevents short circuits. Challenges in laser-based cutting processes arise from the differences in the absorption behavior of the materials in the coating system. If the absorption of the isolation

Table 2: Examples of the TRUMPF TruMicro laser portfolio operating at $\lambda = 515\,\text{nm}$ with relevant specifications.[39]

	TruMicro 2230	**TruMicro 6220**
Wavelength	515 nm	515 nm
Average power (max)	10 W	100 W
Advanced pulse on demand	up to 2 MHz	up to 2 MHz
Repetition rate (max., single pulse picking)	2 MHz	2 MHz
Pulse energy (max.)	40 µJ (at 250 kHz)	100 µJ
Burst patterns	up to 8	up to 16
Burst energy (max.)	100 µJ	1.6 mJ
Pulse duration	< 350 fs	850 fs
Beam quality	$M^2 < 1.3$	$M^2 < 1.3$

layer is too low, the radiation propagates partially to the aluminum and is typically strongly absorbed at the interface. The confined pressure caused by the aluminum ablation leads to material bulging and ultimately to delamination, especially if the coating is very thin. The isolator thus loses its effectiveness. This process is at hand if 1-µm-wavelength pulses are applied to the coated aluminum which is confirmed by the height profile measured by a laser scanning microscope (LSM), see subfigure (b). Switching the wavelength to 515 nm leads to a completely different absorption behavior and, thus, a successful cutting, see subfigure (c). Here, the LSM metrology demonstrates an efficient ceramic ablation process using the same process parameters as for the IR case (pulses of 800 fs duration and of 2.5 µJ energy at a repetition rate of 6 MHz with a feed rate of 2 m/s). The ablated groove exhibits minor bulging at the edges and the cross section at the notching contour is free of delamination.

Specifications of the TRUMPF TruMicro laser portfolio operating at $\lambda = 515\,\text{nm}$ are listed in Table 2 including available parameters for a 100-W-average power laser (TruMicro 6220).

4. MICROMACHINING WITH 343 NANOMETER PULSES

One option to efficiently generate the third harmonic from the primary 1-µm, ytterbium-based ultrafast laser is sum-frequency generation in LBO (lithium triborate) crystals. Here, two intense input signals at frequencies ω_1, ω_2 can generate a third frequency ω_3. For the special case that $\omega_2 = 2\omega_1$, thus, that primary radiation and its second harmonic is at hand, cf. Sec. 3, frequency tripling is achieved ($\omega_3 = 3\omega_1$). Typical conversion efficiencies amount to $> 30\,\%$ for setups employing two LBO crystals with different phase matching conditions in series.[41,50] Here too, external frequency conversion after the amplifier allows the flexibility of the laser system to be maintained, particularly with regard to temporal pulse control.[43] The primary source is actively controlled from the monitored UV signal.

Ultrashort laser pulses at wavelengths of 343 nm represent even more subtle photonic tools than their infrared or green counterparts, cf. Secs. 2 and 3. The corresponding photon energy ensures already a significant linear absorption for many materials being transparent in the visible range, such as polymers[51] and many common glasses.[52] Thus, required fluences for triggering a specific light-matter interaction are low, as is the induced stress to the materials. From a machining perspective, the main application is therefore found in the processing of materials reacting sensitively to thermal loads, such as, e.g., thin polyimides (PI) foils. Ablation of polymers with short and ultrashort UV pulses is a topic that has been worked on for decades,[53,54] driven by the availability of excimer lasers and is currently becoming topical again due to the demand from the consumer electronics industry for polarizing foils or semi-permeable membranes.

Figure 6 depicts the backside of a processed 20-µm-thick polymer film exhibiting sub-2-µm-holes from a percussion drilling strategy with sub-picosecond-pulses emerging from a TruMicro 6320 laser. The focusing is realized with a conventional f-θ-lens of 65 mm effective focal length employing an effective (Gaussian) NA of

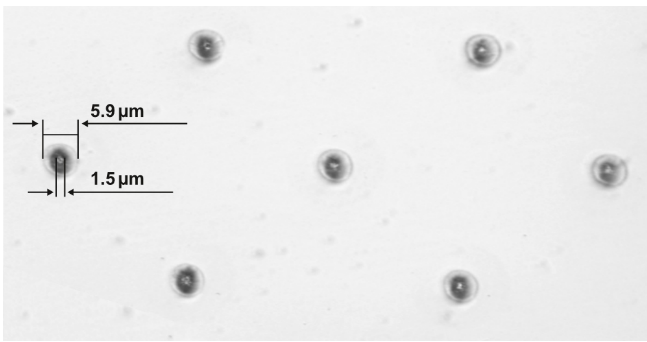

Figure 6: Percussion drilling in a polymer film of $\sim 20\,\mu$m thickness with UV pulses and a standard optical head with effective focal length of $f = 65$ mm. The light micrograph shows the film's backside with hole diameters of 1.5 µm and smallest heat-affected zones.

Table 3: Examples of the TRUMPF TruMicro laser portfolio operating at $\lambda = 343$ nm with relevant specifications.[39]

	TruMicro 6320	**TruMicro 6330**
Wavelength	343 nm	343 nm
Average power (max)	62.5 W	50 W
Advanced pulse on demand	up to 2 MHz	up to 2 MHz
Repetition rate (max., single pulse picking)	3 MHz	3 MHz
Pulse energy (max.)	62.5 µJ	62.5 µJ
Burst patterns	up to 16	up to 8
Burst energy (max.)	800 µJ	500 µJ
Pulse duration	< 850 fs	< 500 fs
Beam quality	$M^2 < 1.3$	$M^2 < 1.3$

< 0.1. In order to realize comparable focus dimensions in the IR, already complex mid-NA microscope objectives are required[31] with significant disadvantages regarding working distance and high-power suitability. However, UV pulses of the same transverse dimension have a threefold longer Rayleigh length as $z_{\mathrm{R}} \sim 1/\lambda$, which leads to a favorable in-volume energy deposition, smaller heat-affected zones and a more robust longitudinal focus positioning tolerance. In the present case, a visible heat-affected zone equals approximately the focus diameter of $\sim 6\,\mu$m, see Fig. 6. For generating the through holes via percussion drilling a set of ~ 10 pulses of $\sim 1\,\mu$J energy is required. Hence, with a single-pulse processing strategy only a fraction of the available pulse energy could be converted. An efficient, industry-relevant process that fully utilizes the energy performance of the source would therefore have to apply beam splitting concepts to increase throughput and to scale the membrane fabrication to macroscopic dimensions,[20] cf. Sec. 2.

Specifications for industrial ultrafast lasers emitting pulses at 343 nm wavelength are shown in Table 3 including information about a 62.5 W-average power version (TruMicro 6320).

5. MICROMACHINING WITH 257 NANOMETER PULSES

Given the broad spectrum of applications and the commercial success of UV ultrafast lasers, it is straightforward to consider the potential of even shorter wavelengths. As an option to generate the fourth harmonic of the primary 1-µm, ytterbium-based laser, two frequency-doubling stages, for example, using one LBO (lithium triborate) crystal and a second BBO (barium borate) crystal including phase-matching management can be employed.[42] Achieved conversion efficiency records amount to $\sim 30\,\%$.[16,55] As with the two frequency conversions discussed before, cf. Secs. 3 and 4, the high stability of DUV radiation is ensured by the fact that the primary laser is controlled by the signal after generating the fourth harmonic.

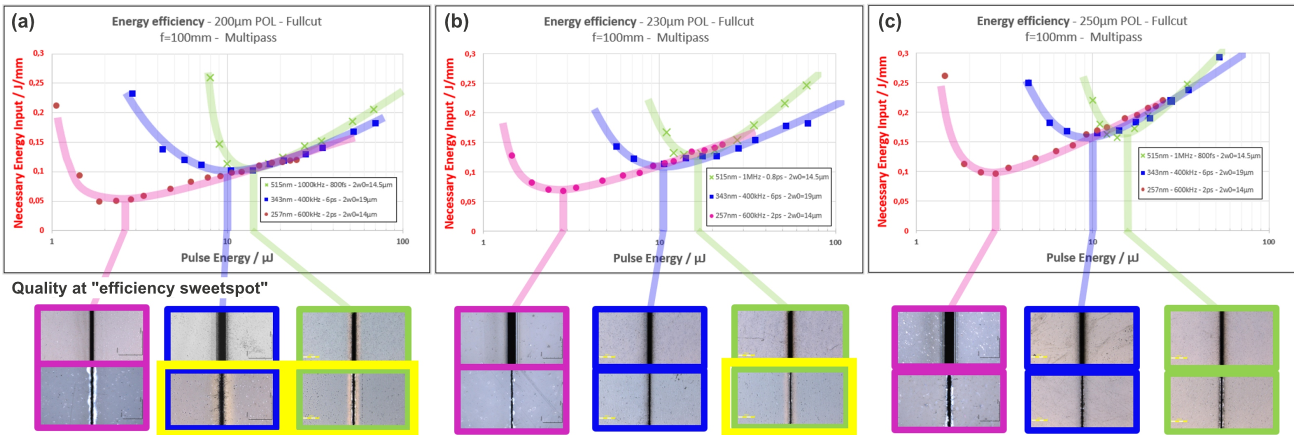

Figure 7: Polymer film cutting of different thicknesses with ultrashort pulse lasers operating at three different wavelengths (green, UV, DUV). The required deposited energy per millimeter for a full cut is plotted as function of pulse energy and wavelength for film thicknesses of 200 µm (a), 230 µm (b) and 250 µm (c). The processing results (entry and exit sides) are shown as light micrographs on the bottom with visible "yellow bands" indicating heat affection, highlighted with yellow boxes.[16]

In theory, the advantages of laser radiation at $\lambda \cong 257$ nm (DUV) are again obvious (even smaller foci, smaller heat-affected zones, etc., cf. Sec. 1). However, DUV radiation presents the user with considerable challenges, so that the industrial use of these lasers is still in its infancy. On the one hand, optics, especially the coatings of transmissive components in this wavelength range, suffer from laser-induced contamination and the effect of UV fatigue, which significantly reduces their service life.[56] On the other hand, DUV scattered light causes eye damage and skin cancer, so that high protective measures must be taken, such as full-body protection.

Despite the challenges described, DUV laser material processing strategies suitable for industrial use have already been demonstrated. As explained in the previous section, it is precisely those processes in which the materials are subjected to the lowest possible thermal stress that benefit, such as thin polymer films acting as polarizers for displays. With Fig. 7, we are analyzing the energy footprint when cutting polarizer films of different thicknesses: 200 µm (a), 230 µm (b) and 250 µm (c). In all three cases the required energy per length is plotted as a function of pulse energy and wavelength (green, UV, DUV). The minimum required energy line density to completely cut through the test foil, is fairly similar for the green and the UV, respectively—both at about 0.1 J/mm. However, taking into account that frequency conversion from IR to green is more efficient than from IR to UV, processing with green lasers is more productive. On the other hand, UV cutting already shows a quality enhancement, see e.g., bottom of subfigure (b) with a visible "yellow band" at the exit side of the 230-µm-thick sample processed with the green laser. Considering the results achieved from the DUV laser the required energy density is a factor of two lower than for the UV/green cases for all three sample thicknesses. Consequently, the deposited heat to the foil is also reduced. However, the local minima of the efficiency curves can be found at a single-pulse energy even reduced by a factor of 5 in comparison to processing with the two other wavelengths. This energy benefit could be invested in higher repetition rates and, thus, in higher feed rates or scanning speeds. Twice the efficiency at a fifth of the pulse energy means a factor of $\sim (2 \ldots 3)$ higher repetition rates at the same IR power (taking the conversion efficiency into account) and the same cutting speed. Again, due to the reduced heat-load applied to the polymer film a quality enhancement is expected, which is confirmed by light microscopy (in particular) of the film's backside, see bottom row of Fig. 7 (a) – (c). Here, the yellow band effect is avoided in all three thickness cases only for the machining with DUV pulses.

Specifications for TRUMPF industrial ultrafast lasers emitting pulses at 257 nm wavelength are shown in Table 4.

Table 4: Examples of available TRUMPF TruMicro laser sources with DUV conversion operating at $\lambda = 257\,\text{nm}$ with relevant specifications.[39]

	TruMicro Mark 1020 + DUV (available upon request)	**TruMicro 6420**
Wavelength	257 nm	257 nm
Average power (max)	1.5 W	10 W
Advanced pulse on demand	yes	yes
Rep. rate (max., single pulse picking)	2 MHz	2 MHz
Pulse energy (max.)	1.5 µJ	12.5 µJ
Pulse duration	< 900 fs	< 850 fs
Beam quality	$M^2 < 1.3$	$M^2 < 1.3$

6. MICROMACHINING WITH 1980 NANOMETER PULSES

Ultrashort pulsed lasers that emit radiation at 2 µm wavelength could become highly relevant for future production strategies, as many semiconductor materials are transparent in this spectral range. Analog to glass processing with 1-µm-ultrafast lasers,[13] in-volume modifications inside silicon generated from nonlinear absorption could form the basis for welding, cutting or waveguide writing.[57,58]

Using thulium-based fiber lasers, high-average and high-peak-power radiation has already been efficiently generated at wavelengths centered around 1980 nm without the need for postconversion from optical parametric amplification.[59–61] Similar to ytterbium-based laser systems, thulium-doped silica fiber amplifier can be efficiently pumped from 790-nm-laser diodes achieving slope efficiencies of $\sim 70\,\%$, exploiting cross-relaxation processes.[61,62] The broad oscillator and amplifier spectrum allows pulses to be compressed directly to less than 400 fs.[61]

Extensive studies on micromachining in semiconductor materials with ultrashort laser pulses at $\lambda = 1550\,\text{nm}$ show that established concepts for dielectrics processing cannot be directly transferred to, for example, silicon, see Ref. 58. Challenges mainly arise from extreme nonlinear material properties preventing a controlled in-volume energy deposition. This typically causes prefocal absorption, strong filament formation and therefore limits the reachable energy density in the volume. Another obstacle is given by the high (linear) refractive index $n_{\text{Si}}\,(\lambda = 2\,\mu\text{m}) \cong 3.5$[63] which induces spherical aberrations at the air-silicon interface, especially at high numerical apertures.[63] Despite these difficulties, process regimes have been found allowing the ultrafast laser welding of silicon and copper[64] or the waveguide writing in silicon.[65] We therefore see great potential for applications with industrial 2-µm-lasers which is confirmed by our experiment depicted in Fig. 8. Here, an ultrafast thulium-based laser from Active Fiber Systems (member of the TRUMPF group) is used in a pulse duration range between $(0.4 \ldots 650)$ ps at a central wavelength of 1980 nm. One benefit of using this wavelength in comparison to lasers operating at $\lambda = 1550\,\text{nm}$ is that other semiconductor materials with a smaller band gaps, such as germanium,[66] are transparent and, theoretically, allow in-volume processing. For other materials, such as gallium arsenide or indium phosphide, the nonlinear absorption order changes from two- to three-photon absorption, which might help in achieving a spatially confined and high energy density. In our experiment, after being carefully attenuated and polarization controlled, the pulses are focused using an NA-0.85-asphere approx. 200 µm deep into the volume of the crystalline silicon (c-Si). The c-Si sample is moved parallel to the x-axis resulting in periodic material changes with a spatial pitch of 12.5 µm. A broadband light source is illuminating these in-volume modifications imaged onto an indium gallium arsenide (InGaAs) camera. The observation direction is perpendicular to the z-axis which corresponds to the propagation direction of the 1980 nm-pulses, see coordinate system in Fig. 8. Although the microscope images (right-hand-side) only show material changes with weak contrast, they confirm that energy can be deposited in the volume and modifications can be generated with the employed laser system. However, spatially confined modifications have been achieved only with comparatively long pulses of 650 ps duration and of single-digit microjoule energy. The high intensities from shorter pulse durations, on the other hand, cause strong prefocal absorption and cause detrimental nonlinear propagation effects. The weak modification signals indicate refractive index changes, which in this case, are

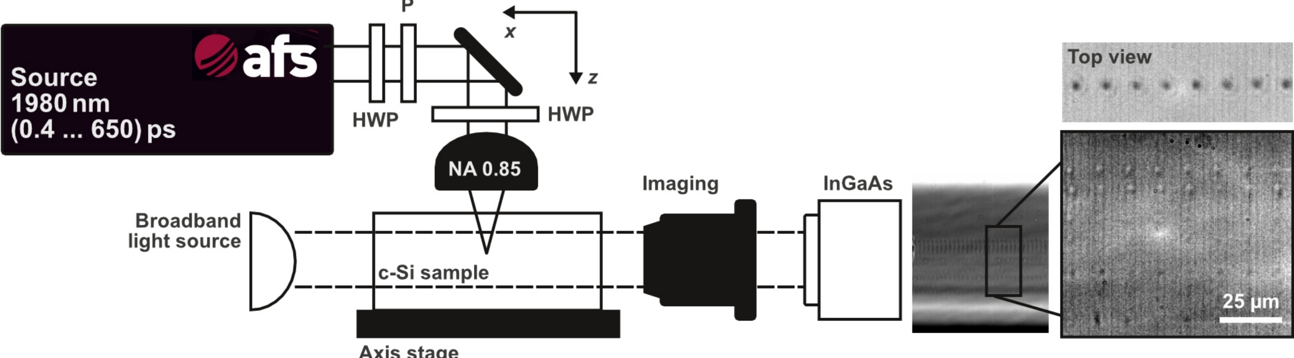

Figure 8: Experimental setup for inducing in-volume modifications in crystalline silicon. Laser pulses at $\lambda =$ 1980 nm central wavelength are focused into the sample and investigated with an imaging setup onto an InGaAs sensor. The micrographs (right-hand-side) confirm a successful energy deposition, see elongated modifications generated from single pulses with 6 µJ energy and 650 ps duration.

Table 5: Specifications of the activeTwo-15 laser from Active Fiber Systems providing ultrashort pulses at a central wavelength of $\lambda = 1980$ nm.[61]

	activeTwo-15
Central wavelength	1980 nm
Average power (max)	15 W
Advanced pulse on demand	yes
Repetition rate (max., single pulse picking)	25 MHz
Pulse energy (max.)	100 µJ
Pulse duration	400 fs ... 1.5 ns
Beam quality	$M^2 < 1.3$

very limited transversely and elongated longitudinally over more than 100 µm. Future investigations will have to show whether stronger modifications can be produced that damage the material and ultimately even enable a separation process.

Table 5 lists important specifications of the activeTwo-15 laser from Active Fiber Systems—a laser which is similar to the one used for in-volume processing of c-Si discussed in this section, but with pulse durations up to 1.5 ns.

7. CONCLUSION

We have reviewed micromachining strategies with ultrafast lasers operating at five different wavelengths spectrally covering almost one order of magnitude. For the laser pulses of different "colors", key applications, such as large-scale metal ablation (IR-1-µm), polymer foil cutting (DUV), or in-volume silicon processing (IR-2-µm) were presented and partially also compared with machining results from other wavelengths. Our review shows that completely new processing strategies can be developed based on the wavelength-degree-of-freedom allowing to control the energy deposition with higher precision. As demonstrated, multilayer systems in particular benefit from processing with higher photon energies. Likewise, the gentle machining of materials being susceptible to thermal stress, such as polymer films, is enabled by shorter wavelengths. Enhanced productivity and quality can often justify the increased expenses related to the frequency conversion or the change of the active medium.

REFERENCES

1. K. C. Phillips, H. H. Gandhi, E. Mazur, and S. Sundaram, "Ultrafast laser processing of materials: a review," *Advances in Optics and Photonics* **7**(4), pp. 684–712, 2015.
2. M. Malinauskas, A. Žukauskas, S. Hasegawa, Y. Hayasaki, V. Mizeikis, R. Buividas, and S. Juodkazis, "Ultrafast laser processing of materials: from science to industry," *Light: Science & Applications* **5**(8), pp. e16133–e16133, 2016.
3. D. Flamm, D. G. Grossmann, M. Sailer, M. Kaiser, F. Zimmermann, K. Chen, M. Jenne, J. Kleiner, J. Hellstern, C. Tillkorn, *et al.*, "Structured light for ultrafast laser micro-and nanoprocessing," *Optical Engineering* **60**(2), p. 025105, 2021.
4. Q. Feng, J. V. Moloney, A. C. Newell, E. M. Wright, K. Cook, P. K. Kennedy, D. Hammer, B. Rockwell, and C. Thompson, "Theory and simulation on the threshold of water breakdown induced by focused ultrashort laser pulses," *IEEE journal of quantum electronics* **33**(2), pp. 127–137, 1997.
5. S. Nolte, C. Momma, H. Jacobs, A. Tünnermann, B. N. Chichkov, B. Wellegehausen, and H. Welling, "Ablation of metals by ultrashort laser pulses," *JOSA B* **14**(10), pp. 2716–2722, 1997.
6. A. Couairon and A. Mysyrowicz, "Femtosecond filamentation in transparent media," *Physics reports* **441**(2-4), pp. 47–189, 2007.
7. B. E. Schmidt, A. Hage, T. Mans, F. Légaré, and H. J. Wörner, "Highly stable, 54mJ Yb-InnoSlab laser platform at 0.5 kW average power," *Optics express* **25**(15), pp. 17549–17555, 2017.
8. C. J. Saraceno, D. Sutter, T. Metzger, and M. A. Ahmed, "The amazing progress of high-power ultrafast thin-disk lasers," *Journal of the European Optical Society-Rapid Publications* **15**(1), p. 15, 2019.
9. M. Müller, C. Aleshire, A. Klenke, E. Haddad, F. Légaré, A. Tünnermann, and J. Limpert, "10.4 kw coherently combined ultrafast fiber laser," *Optics letters* **45**(11), pp. 3083–3086, 2020.
10. A. Gillner, J. Finger, P. Gretzki, M. Niessen, T. Bartels, and M. Reininghaus, "High power laser processing with ultrafast and multi-parallel beams.," *Journal of Laser Micro/Nanoengineering* **14**(2), 2019.
11. D. Flamm, J. Hellstern, A. Heimes, F. Zimmermann, A. Ghazagh, J. Wohletz, F. Kimmich, J. Kleiner, and C. Tillkorn, "Multi-mj ultrafast laser machining with flexible multi-spot patterns," in *High-Power Laser Materials Processing: Applications, Diagnostics, and Systems XI*, **11994**, pp. 146–152, SPIE, 2022.
12. J. Hellstern, C. Tillkorn, T. Hieronymus, M. Kaiser, T. Beck, and D. Flamm, "Optical tools for laser machining along six orders of magnitude," in *High-Power Laser Materials Processing: Applications, Diagnostics, and Systems XIII*, **12878**, p. 1287802, SPIE, 2024.
13. M. Kumkar, M. Kaiser, J. Kleiner, D. Grossmann, D. Flamm, K. Bergner, and S. Nolte, "Ultrafast laser processing of transparent materials supported by in-situ diagnostics," in *Laser Applications in Microelectronic and Optoelectronic Manufacturing (LAMOM) XXI*, **9735**, p. 97350P, International Society for Optics and Photonics, 2016.
14. D. Grossmann, M. Reininghaus, C. Kalupka, M. Kumkar, and R. Poprawe, "Transverse pump-probe microscopy of moving breakdown, filamentation and self-organized absorption in alkali aluminosilicate glass using ultrashort pulse laser," *Optics Express* **24**(20), pp. 23221–23231, 2016.
15. K. Bergner, D. Flamm, M. Jenne, M. Kumkar, A. Tünnermann, and S. Nolte, "Time-resolved tomography of ultrafast laser-matter interaction," *Optics Express* **26**(3), pp. 2873–2883, 2018.
16. S. Häfner, C. Wagner, B. Shnirman, M. Ginter, J. Brons, M. Sailer, A. Fehrenbacher, D. Grossmann, D. Flamm, K. Janami, *et al.*, "Deep uv for materials processing based on the industrial trumicro series of ultrafast solid-state laser amplifiers," in *Nonlinear Frequency Generation and Conversion: Materials and Devices XX*, **11670**, p. 116701F, SPIE, 2021.
17. A. Wetzig, P. Herwig, J. Hauptmann, C. Goppold, R. Baumann, A. Fürst, M. Rose, T. Pinder, A. Mahrle, and E. Beyer, "Latest developments of laser cutting," in *International Congress on Applications of Lasers & Electro-Optics*, AIP Publishing, 2016.
18. T. Fan, "Heat generation in nd: Yag and yb: Yag," *IEEE Journal of Quantum Electronics* **29**(6), pp. 1457–1459, 1993.
19. D. H. Sutter, T. Dietz, D. Bauer, R. Scelle, A. Budnicki, A. Killi, M. Jenne, J. Kleiner, D. Flamm, M. Sailer, *et al.*, "High power and high energy ultrafast disk lasers for industrial applications," in *CLEO: Applications and Technology*, pp. JM3E–2, Optica Publishing Group, 2019.

20. M. Kumkar, M. Kaiser, J. Kleiner, D. Flamm, D. Grossmann, K. Bergner, F. Zimmermann, and S. Nolte, "Throughput scaling by spatial beam shaping and dynamic focusing," in *Laser Applications in Microelectronic and Optoelectronic Manufacturing (LAMOM) XXII*, **10091**, p. 100910G, International Society for Optics and Photonics, 2017.
21. D. C. Mathews, J. Wang, M. Kaiser, M. Kumkar, J. Hellstern, J. Kleiner, and D. Flamm, "Photonic shaping tools for large-scale micro-machining," in *Laser-based Micro-and Nanoprocessing XVIII*, **12873**, pp. 23–33, SPIE, 2024.
22. J. Wang, A. Ghazagh, S. S. Ravi, S. Baumbach, B. Dannecker, M. Scharun, D. Bauer, S. Nolte, and D. Flamm, "Phase retrieval algorithm applied to high-energy ultrafast lasers," *Applied Optics* **63**(10), pp. 2518–2527, 2024.
23. M. Jenne, D. Flamm, K. Chen, M. Schäfer, M. Kumkar, and S. Nolte, "Facilitated glass separation by asymmetric Bessel-like beams," *Optics Express* **28**(5), pp. 6552–6564, 2020.
24. C. Zwahr, N. Serey, L. Nitschke, C. Bischoff, U. Rädel, A. Meyer, P. Zhu, and W. Pfleging, "Targeting new ways for large-scale, high-speed surface functionalization using direct laser interference patterning in a roll-to-roll process," *International Journal of Extreme Manufacturing* **5**(3), p. 035006, 2023.
25. K. Chen, M. Jenne, D. G. Grossmann, and D. Flamm, "Generalized axicon-based generation of nondiffracting beams," *arXiv preprint arXiv:1911.03103* , 2019.
26. F. Wyrowski, H. van Esdonk, R. J. Zuidema, S. Wadmann, and G. J. Notenboom, "Use of diffractive optics in material processing," in *Diffractive and Holographic Optics Technology*, **2152**, pp. 139–144, International Society for Optics and Photonics, 1994.
27. O. Hofmann, J. Stollenwerk, and P. Loosen, "Design of multi-beam optics for high throughput parallel processing," *Journal of Laser Applications* **32**(1), 2020.
28. P. Hauschwitz, B. Stoklasa, J. Kuchařík, H. Turčičová, M. Písařík, J. Brajer, D. Rostohar, T. Mocek, M. Duda, and A. Lucianetti, "Micromachining of invar with 784 beams using 1.3 ps laser source at 515 nm," *Materials* **13**(13), p. 2962, 2020.
29. F. Yu, P. Li, H. Shen, S. Mathur, C.-M. Lehr, U. Bakowsky, and F. Mücklich, "Laser interference lithography as a new and efficient technique for micropatterning of biopolymer surface," *Biomaterials* **26**(15), pp. 2307–2312, 2005.
30. A. F. Lasagni, C. Gachot, K. E. Trinh, M. Hans, A. Rosenkranz, T. Roch, S. Eckhardt, T. Kunze, M. Bieda, D. Günther, *et al.*, "Direct laser interference patterning, 20 years of development: from the basics to industrial applications," in *Laser-based micro-and nanoprocessing XI*, **10092**, pp. 186–196, SPIE, 2017.
31. D. Flamm, J. Hellstern, M. Kaiser, M. Kahmann, J. Kleiner, and C. Tillkorn, "Light along curves: Photonic shaping tools," *Adv. Opt. Techn.* **12**, 2023.
32. D. Flamm, M. Kaiser, M. Feil, M. Kahmann, M. Lang, J. Kleiner, and T. Hesse, "Protecting the edge: Ultrafast laser modified C-shaped glass edges," *Journal of Laser Applications* **34**(1), p. 012014, 2022.
33. J. Dominik, J. Jaksic, K. Ertel, B. Dannecker, M. Scharun, S. Nagel, S. Klingebiel, T. Vogel, C. Saraceno, T. Metzger, *et al.*, "Thin-disk multipass amplifier for 100 mj class, multi-kw high intensity lasers," in *High Intensity Lasers and High Field Phenomena*, pp. HW4B–4, Optica Publishing Group, 2022.
34. C. Tillkorn, A. Heimes, D. Flamm, S. Dorer, T. Beck, J. Hellstern, F. Marschall, and C. Lingel, "Anamorphic beam shaping for efficient laser homogenization: methods and high power applications," in *Laser Resonators, Microresonators, and Beam Control XX*, **10518**, pp. 229–240, SPIE, 2018.
35. L. Romero and F. Dickey, "Lossless laser beam shaping," *JOSA A* **13**(4), pp. 751–760, 1996.
36. W. Choi, H. Y. Kim, J. W. Jeon, W. S. Chang, and S.-H. Cho, "Vibration-assisted femtosecond laser drilling with controllable taper angles for amoled fine metal mask fabrication," *Materials* **10**(2), p. 212, 2017.
37. D. H. Sutter, U. Quentin, F. Kanal, H.-J. Otto, J. Dolkemeyer, R. Gebs, M. Sailer, J. Kleiner, A. Budnicki, C. Schnitzler, *et al.*, "Next generation of high-power industrial ultrafast lasers based on innoslab technology (conference presentation)," in *Solid State Lasers XXIX: Technology and Devices*, **11259**, p. 112591C, SPIE, 2020.
38. L. Büsing, A. Ostendorf, and P. Loosen, "Optische Systeme für die hochpräzise, scannerbasierte Multistrahlbearbeitung mit ultrakurzen Laserpulsen," tech. rep., RWTH Aachen, Lehrstuhl für Technologie optischer Systeme, 2016.

39. "TRUMPF short and ultrashort pulse lasers." https://www.trumpf.com/en_INT/products/lasers/short-and-ultrashort-pulse-laser/. Accessed: 2025-01-22.
40. "RP Photonics Encyclopedia: Frequency doubling." https://www.rp-photonics.com/frequency_doubling.html. Accessed: 2025-01-10.
41. J.-P. Negel, A. Loescher, A. Voss, D. Bauer, D. Sutter, A. Killi, M. A. Ahmed, and T. Graf, "Ultrafast thin-disk multipass laser amplifier delivering 1.4 kW (4.7 mJ, 1030 nm) average power converted to 820 W at 515 nm and 234 W at 343 nm," *Optics express* **23**(16), pp. 21064–21077, 2015.
42. K. Liu, H. Li, S. Qu, H. Liang, Q. J. Wang, and Y. Zhang, "20 W, 2 mJ, sub-ps, 258 nm all-solid-state deep-ultraviolet laser with up to 3 GW peak power," *Optics Express* **28**(12), pp. 18360–18367, 2020.
43. A. Fehrenbacher, M. Sailer, B. Fuehra, F. Jansen, C. Tan, S. Baumbach, R. Flaig, C. Eberhardt, S. Ruebling, U. Quentin, *et al.*, "New generation TruMicro series 2000: micromachining versatility by GHz-burst, higher average power, flexible pulse on demand and integrated hollow-core fiber interface," in *Laser-based Micro- and Nanoprocessing XV*, **11674**, pp. 139–148, SPIE, 2021.
44. L. Tunna, A. Kearns, W. O'neill, and C. Sutcliffe, "Micromachining of copper using nd: Yag laser radiation at 1064, 532, and 355 nm wavelengths," *Optics & Laser Technology* **33**(3), pp. 135–143, 2001.
45. D. Flamm and J. Kleiner, "Laser processing of a partly transparent workpiece using a quasi-non-diffractive laser beam," June 09 2023. Patent Application US20230311245.
46. A. Alwaidh, M. Sharp, and P. French, "Laser processing of rigid and flexible pcbs," *Optics and Lasers in Engineering* **58**, pp. 109–113, 2014.
47. M. Gaidys, A. Žemaitis, P. Gečys, and M. Gedvilas, "Efficient picosecond laser ablation of copper cylinders," *Applied Surface Science* **483**, pp. 962–966, 2019.
48. E. Bez, M. Himmerlich, P. Lorenz, M. Ehrhardt, A. G. Gunn, S. Pfeiffer, M. Rimoldi, M. Taborelli, K. Zimmer, P. Chiggiato, *et al.*, "Influence of wavelength and accumulated fluence at picosecond laser-induced surface roughening of copper on secondary electron yield," *Journal of Applied Physics* **133**(3), 2023.
49. X. Wang and H. Zheng, "High quality laser cutting of electronic printed circuit board substrates," *Circuit World* **35**(4), pp. 46–55, 2009.
50. P. Zhu, D. Li, Q. Liu, J. Chen, S. Fu, P. Shi, K. Du, and P. Loosen, "39.1 μJ picosecond ultraviolet pulses at 355 nm with 1 MHz repeat rate," *Optics letters* **38**(22), pp. 4716–4718, 2013.
51. M.-D. Damaceanu, R.-D. Rusu, M. Bruma, and B. Jarzabek, "Photo-optical properties of poly (oxadiazole-imide) s containing naphthalene rings," *Polymer journal* **42**(8), pp. 663–669, 2010.
52. M. Rubin, "Optical properties of soda lime silica glasses," *Solar energy materials* **12**(4), pp. 275–288, 1985.
53. J. Yeh, "Laser ablation of polymers," *Journal of Vacuum Science & Technology A: Vacuum, Surfaces, and Films* **4**(3), pp. 653–658, 1986.
54. P. Dyer, "Excimer laser polymer ablation: twenty years on," *Applied Physics A* **77**, pp. 167–173, 2003.
55. Q. Fu, N. Hanrahan, L. Xu, S. Lane, D. Lin, Y. Jung, S. Mahajan, and D. J. Richardson, "High-power, high-efficiency, all-fiberized-laser-pumped, 260-nm, deep-UV laser for bacterial deactivation," *Optics Express* **29**(26), pp. 42485–42494, 2021.
56. B. M. Arnold, C. Rashvand, L. Willis, and M. Dabney, "Uv fatigue of laser optics: laser-induced contamination," in *Laser-Induced Damage in Optical Materials 2022*, **12300**, pp. 77–84, SPIE, 2022.
57. M. Chanal, V. Y. Fedorov, M. Chambonneau, R. Clady, S. Tzortzakis, and D. Grojo, "Crossing the threshold of ultrafast laser writing in bulk silicon," *Nature communications* **8**(1), p. 773, 2017.
58. M. Chambonneau, D. Grojo, O. Tokel, F. Ö. Ilday, S. Tzortzakis, and S. Nolte, "In-volume laser direct writing of silicon—challenges and opportunities," *Laser & Photonics Reviews* **15**(11), p. 2100140, 2021.
59. F. Stutzki, C. Gaida, M. Gebhardt, F. Jansen, A. Wienke, U. Zeitner, F. Fuchs, C. Jauregui, D. Wandt, D. Kracht, *et al.*, "152 w average power tm-doped fiber cpa system," *Optics letters* **39**(16), pp. 4671–4674, 2014.
60. C. Gaida, M. Gebhardt, T. Heuermann, F. Stutzki, C. Jauregui, and J. Limpert, "Ultrafast thulium fiber laser system emitting more than 1 kW of average power," *Optics letters* **43**(23), pp. 5853–5856, 2018.
61. C. Gaida, T. Heuermann, S. Breitkopf, T. Eidam, and J. Limpert, "Industrial-grade 2-μm ultrafast fiber laser CPA for silicon processing: Delivering > 100 μJ pulses at 1980 nm with < 400 fs duration and > 15 W average power," *PhotonicsViews* **21**(5), pp. 44–47, 2024.

62. M. Tao, Q. Huang, T. Yu, P. Yang, W. Chen, and X. Ye, "Cross relaxation in tm-doped fiber lasers," in *2nd International Symposium on Laser Interaction with Matter (LIMIS 2012)*, **8796**, pp. 472–477, SPIE, 2013.
63. M. Chambonneau, M. Blothe, Q. Li, V. Y. Fedorov, T. Heuermann, M. Gebhardt, C. Gaida, S. Tertelmann, F. Sotier, J. Limpert, *et al.*, "Transverse ultrafast laser inscription in bulk silicon," *Physical Review Research* **3**(4), p. 043037, 2021.
64. M. Chambonneau, Q. Li, V. Y. Fedorov, M. Blothe, K. Schaarschmidt, M. Lorenz, S. Tzortzakis, and S. Nolte, "Taming ultrafast laser filaments for optimized semiconductor–metal welding," *Laser & Photonics Reviews* **15**(2), p. 2000433, 2021.
65. M. Blothe, A. Alberucci, N. Alasgarzade, M. Chambonneau, and S. Nolte, "Transverse inscription of silicon waveguides by picosecond laser pulses," *Laser & Photonics Reviews* **18**(11), p. 2400535, 2024.
66. C. G. Van de Walle, "Band lineups and deformation potentials in the model-solid theory," *Physical review B* **39**(3), p. 1871, 1989.